I-EDU GROUP

Article

Optical properties of 2D Dirac materials (BeN_4, IrN_4, MgN_4, PtN_4 and RhN_4): a density functional theory study

Gofur B. Eshonqulov[1], Anora Meylieva [1], Golibjon R. Berdiyorov *[2]

[1] Department of Physics, National University of Uzbekistan, Tashkent, 100174, Uzbekistan
[2] Qatar Environment and Energy Research Institute, Hamad Bin Khalifa University, Doha, 34110, Qatar
g.eshonqulov@nuu.uz (G.E.), gberdiyorov@hbku.edu.qa (G.B.)
* Correspondence: gberdiyorov@hbku.edu.qa; Tel: +974 44546704

Abstract: Using density functional theory calculations, the optical properties of recently discovered 2D Dirac materials BeN_4, IrN_4, MgN_4, PtN_4, and RhN_4 were examined. The study revealed that the metallic components significantly influence the electronic and optical properties of these materials. For instance, the absorption spectra of the experimentally synthesized material BeN_4 can be increased by more than three orders of magnitude in the broad spectral range by substituting Be atoms with other metallic atoms such as Rh. This enhanced absorption is attributed to the substantial contribution of the metal atoms to the density of states of the system. Other optical parameters, such as refractive index and reflectivity, are also modified by the replacement of metal atoms. These findings highlight the possibility of manipulating the optical properties of such low-dimensional materials through metal atom substitutions.

Keyword: dirac material, metal doping, electronic transport.

Introduction

Low-dimensional Dirac materials present a great potential for nanoelectronics applications due to their exceptional electronic, transport and optical properties [1]. The existence of the Dirac cone (i.e., a Fermi level linear band dispersion) results in interesting phenomena such as quantum Hall effect [2,3]. A first member of a new type of 2D Dirac materials – beryllonitrene (BeN_4) – was recently synthesized, which consisting of a polymeric nitrogen chains with periodic arrangement of Be atoms [4]. Contrary to the other 2D Dirac materials [5–7], this new material has an anisotropic Dirac point and therefore may have different properties such as anisotropic electron mobility [8,9]. Recent first-principles calculations predict the possibility of creating new 2D Dirac materials by replacing Be atoms in BeN_4 by other metal atoms such as Ir, Mg, Pt and Rh [10]. However, the chemical and physical properties of these new materials remain unexplored and therefore require additional research.

In this work, we use density functional theory (DFT) calculations to study the electronic and optical properties of 2D Dirac materials BeN_4, IrN_4, MgN_4, PtN_4, and RhN_4 (see Fig. 1). We found that metal atom replacement results in a considerable increase in absorption across infrared, visible, and UV ranges of the spectrum. In fact, absorption can be enhanced by several orders of magnitude depending on the photon energy. This enhancement originates from the contribution of the metal atom to the density of states (DOS) of the system near the Fermi level. Other optical parameters, such as the refractive index and reflectivity, are also affected by the metal atoms. These findings can be useful in fundamentally understanding the role of metal atoms in the optical properties of such low-dimensional materials.

Quoting: Gofur B.Eshonqulov, Anora Meylieva, Golibjon R.Berdiyorov. Optical properties of 2D Dirac materials (BeN_4, IrN_4, MgN_4, PtN_4 and RhN_4): a density functional theory study. **2025**, 2, 1, 2. https://doi.org/

Received: 10.01.2025
Corrected: 18.01.2025
Accepted: 25.01.2025
Published: 30.01.2025

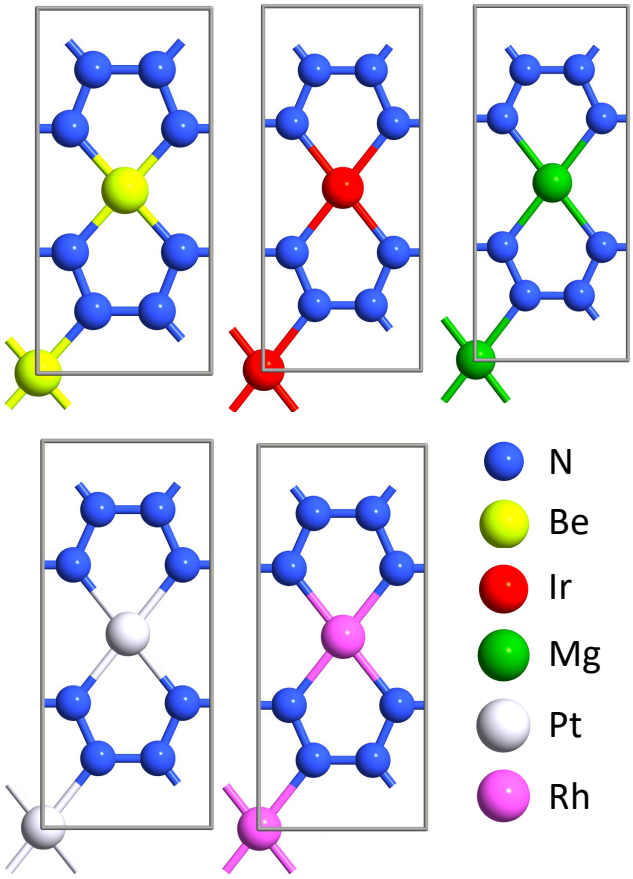

Figure 1. Optimized structures of MN_4 unit cells (M = Be, Ir, Mg, Pt, and Rh).

Materials and Methods

Figure 1 shows optimized structure of the considered 2D materials, which are geometry optimized using periodic boundary conditions using $15\times15\times1$ Monkhorst-Pack k-point sampling [11]. The exchange-correlation is represented by the generalized gradient approximation of Perdew-Burke-Ernzerhof (PBE) [12]. Norm-conserving PseudoDojo pseudopotential with high basis sets is used for all atoms in the system [13] with a real-space grid with mesh cutoff energy of 250 Ry. Grimme's PBE-D empirical dispersion correction [14] was used for van der Waals interactions. The convergence criterion for Hellman-Feynman forces and stress were 0.005 eV/Å and 0.005 GPa, respectively.

Optical properties of the considered systems are obtained from the susceptibility tensors using the Kubo-Greenwood formula:

$$\chi_{i,j}(\omega) = -\frac{e^2\hbar^4}{m^2\varepsilon_0 V\omega^2}\sum_{nm}\frac{f(E_m)-f(E_n)}{E_{nm}-\hbar\omega-i\hbar\Gamma}\pi^i_{nm}\pi^j_{mn}, \tag{1}$$

where f is the Fermi function, π^i_{nm} is the i-component of the dipole matrix element between states n and m, Γ is the broadening and V is the volume. The frequency dependent complex dielectric function $\varepsilon(\omega) = \varepsilon_1(\omega) + i\varepsilon_2(\omega)$ is related to the electric susceptibility as $\varepsilon(\omega) = 1 + \chi(\omega)$ and describes the linear response of the dielectric properties of the material.

The optical conductivity σ and polarizability α are defined as

$$\sigma(\omega) = -i\omega\varepsilon_0\chi(\omega), \tag{2}$$

$$\alpha(\omega) = V\varepsilon_0\chi(\omega). \tag{3}$$

The refractive index n is related to the complex dielectric constant as

$$n + ik = \sqrt{\varepsilon}, \tag{4}$$

where k is the extinction coefficient, which is defines the optical absorption coefficient as

$$\alpha_0 = \frac{2\omega}{c}k. \tag{5}$$

The reflectivity R is given by

$$R = \frac{(1-n)^2 + k^2}{(1+n)^2 + k^2}. \tag{6}$$

Calculations are conducted using the computational package Atomistix toolkit [15,16].

Results

Table 1. Lattice parameters (a and b) and nitrogen-metal atom distance (d) for the considered materials.

System	a(Å)	b(Å)	d(Å)
BeN_4	3.664	7.736	1.748
IrN_4	3.762	8.684	1.959
MgN_4	3.857	8.939	2.052
PtN_4	3.792	8.703	1.980
RhN_4	3.769	8.687	1.970

The study begins with an analysis of structural changes resulting from metal atom replacement. Table I displays the parameters (a and b) of the simple orthorhombic lattice and the distance between the metal atom and the nitrogen (d). The data indicate that the lattice parameters increase upon replacing the Be atoms with any of the considered metal atoms. The largest cell parameters are observed for the MgN_4 system, which also exhibits the greatest distance d. Despite these changes, the system maintains its planar structure in all cases.

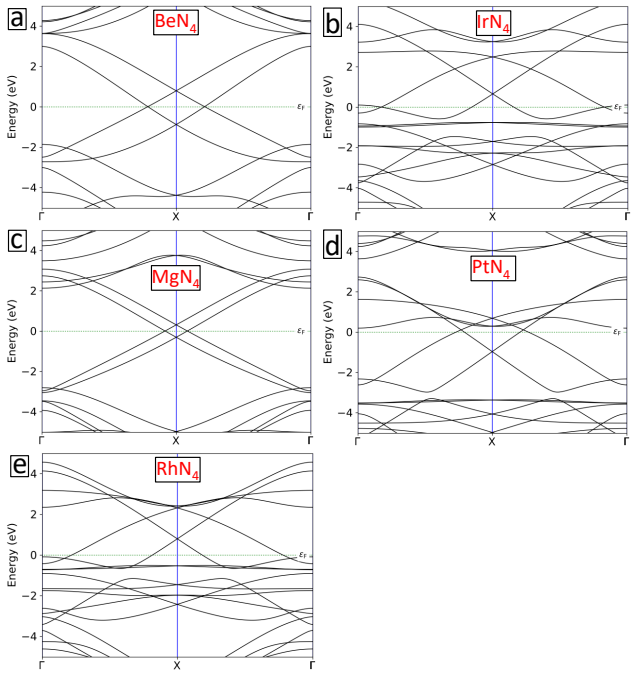

Figure 2. Electronic band structure of BeN_4 (a), IrN_4 (b), MgN_4 (c), PtN_4 (d) and RhN_4 (e).

Next, we study how the inclusion of different metal atoms affects the electronic properties of the 2D material. Figure 2 presents the electronic band structure of the materials along key symmetry points in the Brillouin zone. As expected, the reference system shows a characteristic linear band crossing at the Fermi level, indicating the presence of Dirac cones, which is typical for 2D Dirac materials (see Fig. 2 (a)). This result serves as a baseline for comparison. For the IrN_4 (Fig. 2 (b)), MgN_4 (Fig. 2 (c)), and PtN_4 (Fig. 2 (d)) samples, similar band structures are observed, with linear band crossings occurring near the Fermi level. The key difference among these systems lies in the symmetry points where the crossings occur, reflecting subtle variations in the electronic structure introduced by the different metal atoms. Despite these shifts, the Dirac-like behavior is preserved, confirming that these metal substitutions do not significantly alter the semimetallic character of the material. However, a distinct feature is observed in the RhN_4 sample (Fig. 2 (e)), where the band crossing is shifted slightly below the Fermi level. This shift suggests a minor modification in the electronic behavior, potentially introducing a small gap or altering the material's transport properties at the Fermi level. Such changes could have significant implications for practical applications, where fine-tuning of the electronic structure is desirable. Overall, the results highlight that while the general Dirac nature of the electronic bands is maintained across all metal substitutions, the exact positioning of the band crossings and their relationship to the Fermi level can be controlled by the choice of metal atom. These findings are in good agreement with the previous work of Mortazavi et al. [10], further validating the robustness of the computational models used in this study.

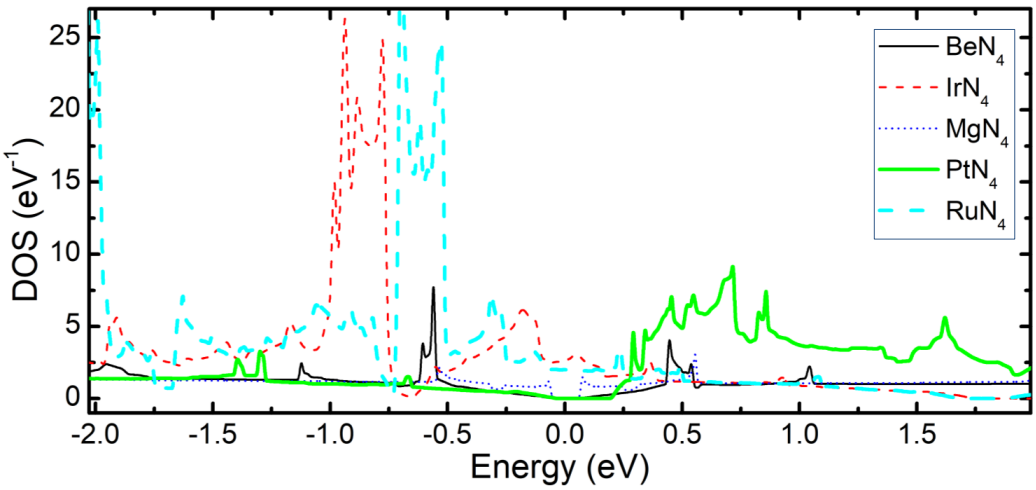

Figure 3. Density of states of the considered samples (zero corresponds to the Fermi energy).

Figure 3 illustrates the density of states (DOS) of the systems as a function of electron energy, with zero corresponding to the Fermi level. The DOS for the reference material BeN_4 (represented as a thin-solid-black curve) shows a relatively flat distribution across the energy spectrum, marked by minor peaks away from the Fermi level. The introduction of different metal atoms, such as Ir, Pt, and Ru, results in a pronounced increase in the DOS within the explored energy ranges. Notable peaks for Ir, Pt, and Ru indicate a significant enhancement in the electronic states at these energy levels. The variation in the DOS demonstrates that the electronic properties of this 2D material are highly sensitive to the specific metallic components used. The substantial peaks near the Fermi level, particularly for Ir, Pt, and Ru, suggest these metals increase the availability of electronic states, potentially impacting the material's conductivity and other electronic properties.

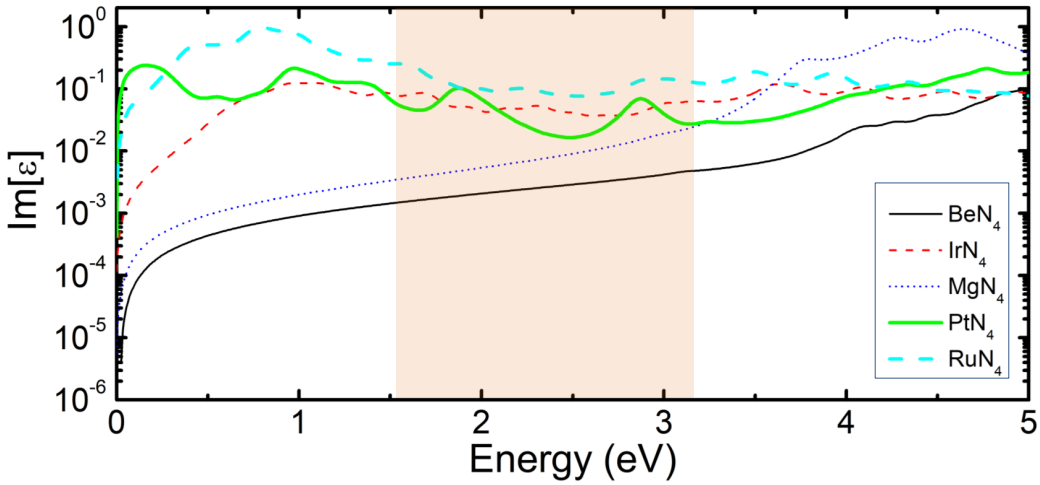

Figure 4. zz-components of the imaginary part of dielectric constant as a function of photon energy for BeN_4, IrN_4, MgN_4, PtN_4 and RhN_4. The visible range of the spectrum is shaded.

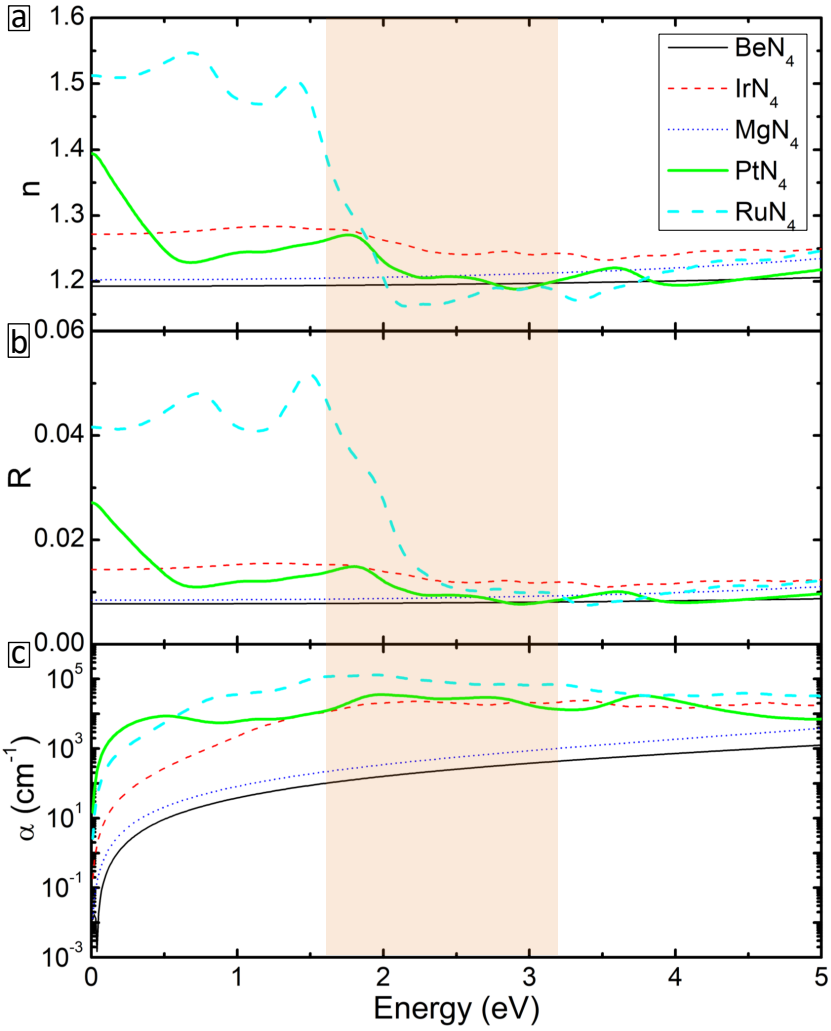

Figure 5. (a) Refractive index, (b) reflectivity and (c) absorption spectra of the considered structures. Only diagonal zz-components of the considered samples are presented.

The analysis proceeds with an examination of the optical properties of the considered 2D systems. For these calculations, a broadening of 0.1 eV was applied to account for thermal effects, and 40 bands both below and above the Fermi level were included in the optical spectrum calculations. Figure 4 shows the imaginary part of the dielectric function, ε, as a function of photon energy for all systems, focusing on the zz-component of the dielectric function. The reference system, represented by a thin-solid-black curve, exhibits a monotonic increase in the imaginary part of ε with increasing photon energy. Substituting Be atoms with Mg atoms results in a slight increase in the imaginary part of ε as shown by the thin-dashed-blue curve. Replacements with other metal atoms lead to further increases in the imaginary part of ε across the entire spectrum, accompanied by fluctuations in the infrared and visible ranges. Notably, the RhN_4 sample, depicted by a thick-dashed-cyan curve, shows the most significant enhancement, which can be more than two orders of magnitude depending on the photon energy value. This pronounced increase highlights the strong influence of metal atom substitutions on the optical characteristics of these materials, suggesting potential applications where enhanced optical properties are crucial.

Figure 5 provides a comprehensive overview of various optical parameters (refractive index n, reflectivity R, and absorption coefficient α) for the studied systems as a function of photon energy. The refractive index of the reference sample, BeN_4, exhibits minimal dependence on photon energy, as shown by the thin-solid-black curve in panel (a). This behavior is similarly observed in the MgN_4 (thin-dotted-blue curve) and IrN_4 (thin-dashed-red curve) samples, albeit with marginally higher values of n. The PtN_4 system displays an increased refractive index compared to the reference in the infrared and certain visible spectral regions (thick-solid-green curve), while the RhN_4 system achieves the highest n at lower photon energies (thick-dashed-cyan curve). However, the refractive index for RhN_4 drops below that of the reference within the visible spectrum. Reflectivity trends for these materials mirror those observed for the refractive index, as illustrated in panel (b). The absorption characteristics, detailed in panel (c), highlight a contrasting behavior. The BeN_4 sample shows the lowest absorption across the spectrum (thin-solid-black curve), with a modest improvement seen with Mg substitution (thin-dotted-blue curve). Substantial enhancements in absorption are evident for the remaining systems across all photon energies, particularly for the RhN_4 system, which shows an increase of more than three orders of magnitude. This analysis underscores how metal atom substitution in BeN_4 significantly improves its optical properties, enhancing parameters like absorption, which are crucial for applications in optoelectronic devices and sensors. The findings suggest potential avenues for tailoring material properties to meet specific technological needs, leveraging the unique responses of these materials to metal substitutions.

Conclusions

Using first-principles density functional theory calculations, we study the structural, electronic and optical properties of BeN_4, IrN_4, MgN_4, PtN_4 and RhN_4 2D Dirac materials. We found that the metal atoms have significant contribution to the electronic structure of the system. Consequently, optical properties of the system can be significantly improved by metal atom replacement. For example, the adsorption spectrum of the material can be increased by several orders of magnitude by replacing Be atoms with Rh atoms in infrared, visible and UV ranges of the spectrum. The ability to fine-tune electronic properties through strategic metal atom substitutions provides a pathway for developing materials tailored for advanced applications in sensors, conductors, and optoelectronic devices, effectively merging multiple functionalities into a single coherent platform for technological innovations.

Authors' contribution.

G.E. and G.B. conceptualized the manuscript, G.B. conducted the simulations, and all authors contributed to the manuscript's preparation and revision.

Funding source.

This research received no external funding.

Ethics approval.

Not required. This study did not include experiments involving humans or animals, so the approval of the ethics committee is not required.

Consent for publication

Not required. The study did not include human participation, therefore, obtaining consent for publication is not required.

Data Availability Statement

Data will be available upon request from the authors.

Acknowledgments

G.E. and A.M. acknowledge the support of the Agency for Innovative Development of the ministry of Higher Education, Science and Innovations.

Conflict of interest

The authors declare no conflicts of interest.

Abbreviations

DFT	Density Functional Theory
DOS	Density of States
PBE	Perdew–Burke–Ernzerhof
GGA	Generalized Gradient Approximation

References

[1] K. S. Novoselov, A. K. Geim, S. V. Morozov, D. Jiang, Y. Zhang, S. V. Dubonos, I. V. Grigorieva, and A. A. Firsov, Electric Field Effect in Atomically Thin Carbon Films, Science 306 (2004) 666-669.

[2] S. A. Yang, Dirac and Weyl Materials: Fundamental Aspects and Some Spintronics Applications, Spin 6 (2016) 1640003.

[3] T. O. Wehling, A. M. Black-Schaffer, and A. V. Balatsky, Dirac materials, Advances in Physics 63 (2014) 1-76.

[4] M. Bykov, T. Fedotenko, S. Chariton, D. Laniel, K. Glazyrin, M. Hanfland, J. S. Smith, V. B. Prakapenka, M. F. Mahmood, A. F. Goncharov, A. V. Ponomareva, F.c Tasnádi, A. I. Abrikosov, T. Bin Masood, I. Hotz, A. N. Rudenko, M. I. Katsnelson, N. Dubrovinskaia, L. Dubrovinsky, and I. A. Abrikosov, High-Pressure Synthesis of Dirac Materials: Layered van der Waals Bonded BeN4 Polymorph, Phys. Rev. Lett. 126 (2021) 175501.

[5] K. S. Novoselov, A. K. Geim, S. V. Morozov, D. Jiang, M. I. Katsnelson, I. V. Grigorieva, S. V. Dubonos, A. A. Firsov, Two-dimensional gas of massless Dirac fermions in graphene, Nature 438 (2005) 197-200.

[6] S. Cahangirov, M. Topsakal, E. Akturk, H. Sahin, S. Ciraci, Two- and One-Dimensional Honeycomb Structures of Silicon and Germanium, Phys. Rev. Lett. 102 (2009) 236804.

[7] M. Neek-Amal, A. Sadeghi, G. R. Berdiyorov, and F. M. Peeters, Realization of free-standing silicene using bilayer graphene Appl. Phys. Lett. 103 (2013) 261904.

[8] S. Banerjee, R. R. P. Singh, V. Pardo, and W. E. Pickett, Tight-Binding Modeling and Low-Energy Behavior of the Semi-Dirac Point, Phys. Rev. Lett. 103 (2009) 016402.

[9] G. R. Berdiyorov, B. Mortazavi, H. Hamoudi, Anisotropic charge transport in 1D and 2D BeN4 and MgN4 nanomaterials: A first-principles study, FlatChem 31 (2022) 100327.

[10] B. Mortazavi, F. Shojaeib and X. Zhuang, Ultrahigh stiffness and anisotropic Dirac cones in BeN_4 and MgN_4 monolayers: A first-principles study, Materials Today Nano (2021) 100125.

[11] H. J. Monkhorst and J. D. Pack, Special points for Brillouin-zone integrations, Phys. Rev. B 13 (1976) 5188.

[12] F. Tran, and P. Blaha, Accurate Band Gaps of Semiconductors and Insulators with a Semilocal Exchange-Correlation Potential, Phys. Rev. Lett., 102 (2009) 226401.

[13] M. J. van Setten, M. Giantomassi, E. Bousquet, M. J. Verstraete, D. R. Hamann, X. Gonze, and G.-M. Rignanese, The pseudodojo: Training and grading a 85 element optimized norm-conserving pseudopotential table, Computer Physics Communications 226 (2018) 39-54.

[14] S. Grimme, Semiempirical GGA-type density functional constructed with a long-range dispersion correction, J. Comp. Chem. 27 (2006) 1787-1799.

[15] S. Smidstrup, T. Markussen, P. Vancraeyveld, J. Wellendorff, J. Schneider, T. Gunst, B. Verstichel, D. Stradi, P. A. Khomyakov, and U. G Vej-Hansen, QuantumATK: An integrated platform of electronic and atomic-scale modelling tools, J. Phys.: Condens. Matter 32 (2020) 015901.

[16] S. Smidstrup, D. Stradi, J. Wellendorff, P. A. Khomyakov, U. G. Vej-Hansen, M-E. Lee, T. Ghosh, E. Jonsson, H. Jonsson, and K. Stokbro, First-principles Green's-function method for surface calculations: A pseudopotential localized basis set approach, Phys. Rev. B 96 (2017) 195309.